Pergamon

Int. J. Mach. Tools Manufact. Vol. 34, No. 8, pp. 1045–1057, 1994

0890–6955/94$7.00 + .00

GRINDABILITY OF SOME METALLIC AND CERAMIC MATERIALS IN CFG REGIMES

L. C. ZHANG†

(*Received* 2 *August* 1993; *in final form* 30 *November* 1993)

Abstract—Creep-feed grinding (CFG) is characterized by large wheel depths of cut and low table speeds and is a process most suitable for geometrical shaping. It also improves the productivity and surface quality for various engineering components with complex profiles. In the last few decades, the application of CFG to metallic materials has been quite successful, but many problems have been encountered in creep-feed grinding ceramics as this kind of material exhibits very different micro- and macro-behaviour. For example, one of the main problems of surface integrity is the micro-cracks induced in the surface and sub-surface of a ground ceramic component, which usually does not take place in grinding metallic materials because of their ductility. Accordingly, manufacturing industries need imperatively practical guidelines to meet various technological requirements in production.

The purpose of this paper is to investigate the grindability of some metallic and ceramic materials through a set of carefully arranged experiments. Wheel depth of cut and table speed are two processing variables for obtaining specific material removal rates. A high carbon chromium bearing steel is chosen to be representative of metallic materials, and the normally sintered SiC and Si_3N_4 are chosen as ceramics. Discussion is focused on the relationships and variation of grinding forces, surface roughness and interface deformation mechanisms. New formulae for modelling grinding forces and surface roughness are successfully proposed. A series of in-depth understanding and useful results for the grindability investigation of different types of materials are provided. The simple relationships obtained in this paper would be very useful for the practical design of industrial grinding operations.

NOMENCLATURE

a	wheel depth of cut
b	the grinding width
D	diameter of the grinding wheel
E_w	elastic modulus of the workpiece material
F	grinding force
H	hardness of the workpiece material
h_{eq}	equivalent chip thickness, defined as $(v_w a/v_s)$
K_{IC}	fracture toughness of the workpiece material
Q	material removal rate
R_a	average roughness of a ground surface, the arithmetic mean of the departures of the profile from the mean line
R_{tm}	the mean of five R_t values obtained in an assessment, where R_t is the maximum peak-to-valley height of the profile in one sampling length
t	grinding time
t_p	bearing ratio of a ground surface
v_s	wheel speed
v_w	table speed
α,β	parameters defined by equation (1)
ζ	parameter defined by equation (2)
ξ	parameter defined by equation (3)

Superscripts

A	along grinding direction
P	perpendicular to the grinding direction

Subscripts

h	horizontal
n	normal direction to the grinding interface
n/t	n or t, see equations (3)–(7)
t	tangential direction to the grinding interface
v	vertical

†Department of Mechanical and Mechatronic Engineering, The University of Sydney, NSW 2006, Australia.

1. INTRODUCTION

CONSIDERABLE work has been carried out in recent years to understand the mechanisms of grinding ductile and brittle materials by regarding the grinding process as an interaction system between the surfaces of the grinding wheel and the workpiece [1–6]. Particular attention has been paid to the improvement of surface integrity and productivity in the creep-feed grinding advanced ceramics. The importance of the CFG process to manufacturing industries lies in that in spite of the development of other machining and processing technologies, it is always required for shaping materials into a specific geometry with desired precision and surface finish. Although the application of CFG to metallic materials has been quite successful, many problems have been encountered in creep-feed grinding ceramics as this kind of material exhibits very different micro- and macro-behaviour. Generally, the principle of the CFG technology is clear and many problems in industrial applications have been summarized in detail in a number of monographs (for example, Andrew *et al.* [2]). However, an investigation into specific parametric relations for practical technological design is still an urgent necessity.

When brittle materials are concerned, the material removal mechanisms of fracture and non-fracture modes need to be addressed particularly [3–6]. A commonly accepted interpretation for obtaining plastically deformed chips from brittle materials is the consideration of material-removal energy [4,7]. It states that when the depth of cut is sufficiently small, plastic flow rather than brittle fracture in a brittle material takes place during the process of material removal when the applied strain exceeds the yield strain of the material but the ratio of the specific work required for cracking to the energy rate in the loaded material keeps bigger than a unit. Unfortunately, such an explanation is quite qualitative and difficult to use in practical applications. Therefore, proper methods for the recognition of brittle- or ductile-mode grinding and an understanding of the behaviour of brittle materials, such as the relationship between the grinding force and some key parameters, need to be explored.

Key factors which control a CFG process could be divided into two groups, the external and internal. The external factors include the wheel surface topography, cooling condition, properties of workpiece materials, and the material removal parameters that involve mainly the wheel depth of cut and the velocities of wheel and workpiece surfaces. The internal factors are the interface temperature, interface forces and the interface deformation, which as a matter of fact, are caused and governed by the external. To investigate a CFG process, a methodology should be designed to analyse the variation mechanisms of internal factors subjected to well-defined and clearly recognized external parameters, so that a useful correlation between them could finally be established.

The purpose of the present paper is to investigate the grindability of some metallic and ceramic materials through a set of carefully arranged experiments. Wheel depth of cut and table speed are two processing variables for obtaining specific material removal rates. A high carbon chromium bearing steel, SUJ2, is chosen to be representative of metallic materials, and the normally sintered SiC and Si_3N_4 are chosen as ceramics. Discussion is focused on the relations and variation of grinding forces, surface roughness and interface deformation mechanisms. The paper provides a series of in-depth insights and useful results for the grindability investigation of different types of materials.

2. EXPERIMENTS

All CFG operations (surface grinding only in this paper) were performed in the down-grinding mode by a modified Jones–Shipman surface grinding machine of model 540CP (the wheelspindle stiffness is 95 N/μm). SUJ2 (a typical high carbon chromium bearing steel), Si_3N_4 and SiC were chosen as specimen materials to reflect the effect of material properties of different classes, where SUJ2 is ductile, and Si_3N_4 and SiC are brittle. It is worthwhile to note, however, that Si_3N_4 is more "ductile" than SiC

with a ratio of fracture toughness being 1–2 times higher (the values of K_{IC} for SiC are 3–4 (MPa $m^{1/2}$) while those for Si_3N_4 are 4–6 (MPa $m^{1/2}$)). Grinding operations were carefully arranged to vary material removal rate, Q, in a wide range by changing table speed and wheel depth of cut alternatively (see the grinding diagrams shown in Fig. 1). The upper Q value is bounded by the onset of workpiece burning under a standard cooling condition. In so doing, the effects of these parameters on the surface finish could be explored to the full extent. Operations under the same conditions were carried out to compare the responses from different wheels and different workpiece materials. Hopefully, such a selection and arrangement of wheels and materials should provide the most useful information. Table 1 presents grinding conditions and Fig. 2 shows details of the grinding wheels used and their structures. Coolant, with a flowrate of 12 l/min, was supplied in a tangential direction only for the HA wheel but in both tangential and radial directions when CBN and MDY (diamond) wheels were used. The velocity of the coolant was 0.44 m/sec in the tangential direction and 1.5 m/sec in the radial direction.

Compared with a conventional grinding process, the contact arc length between the wheel and workpiece in the CFG regime is much longer so that a stringent coolant application is generally required. In recent years, it has been well recognized by production industries that slotted wheels with radial holes (see Fig. 2) could provide a great advantage for bringing adequate coolant into the grinding zone [2, 8], which becomes extremely critical for difficult-to-machine materials. Hence, the CBN and MDY wheels with slotted structures were used in the present study.

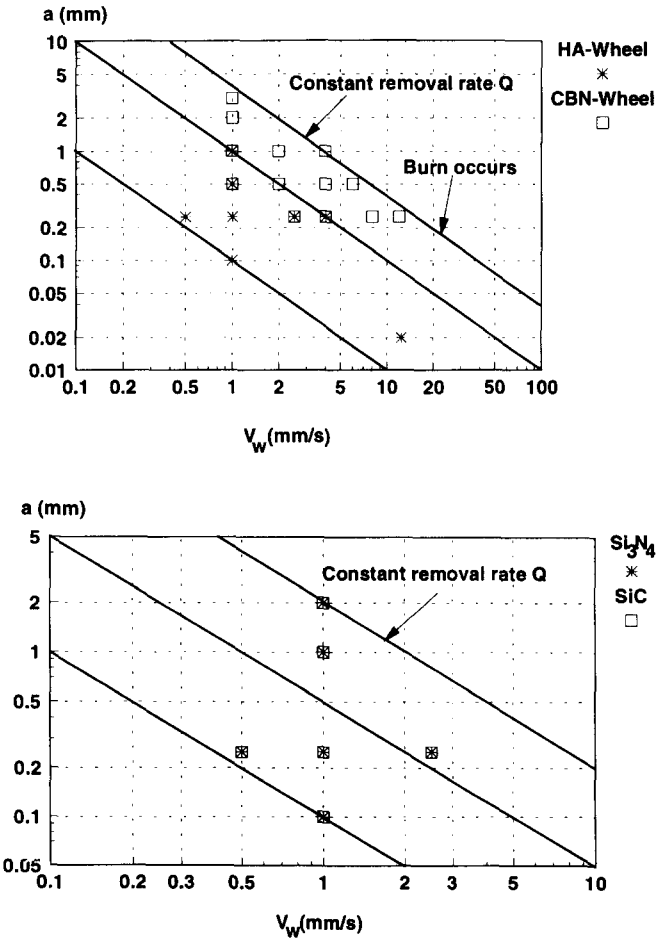

FIG. 1. Grinding diagrams: (a) for SUJ2; (b) for Si_3N_4 and SiC.

TABLE 1. GRINDING CONDITIONS

Workpiece materials	SUJ2 (HRC 60)	Si_3N_4	SiC
Type of grinding wheel	HA60F12VA-2	MDY170/200Q125V	MDY170/200Q125V
	CBN170/200Q125V		
Wheel diameter (mm)	205	205	205
Wheel speed (m/min)	1800	1800	1800
Grinding width (mm)	5	5	5
Table speed (mm/sec)	0.5–12.0	0.5–2.5	0.5–2.5
Wheel depth of cut (mm)	0.02–3.0	0.1–2.0	0.1–2.0
Material removal rate (mm^3/mm sec)	0.1–3.0	0.1–2.0	0.1–2.0
Grinding mode	Down-grinding	Down-grinding	Down-grinding
Coolant (attenuant with water of 20 times)	JIS W 2-No. 2	JIS W 2-No. 2	JIS W 2-No. 2
Coolant velocity (m/sec)	0.44 (in tangential direction only)	0.44 in tangential direction; 1.5 in radial direction	0.44 in tangential direction; 1.5 in radial direction
Coolant flowrate (l/min)	12	12	12

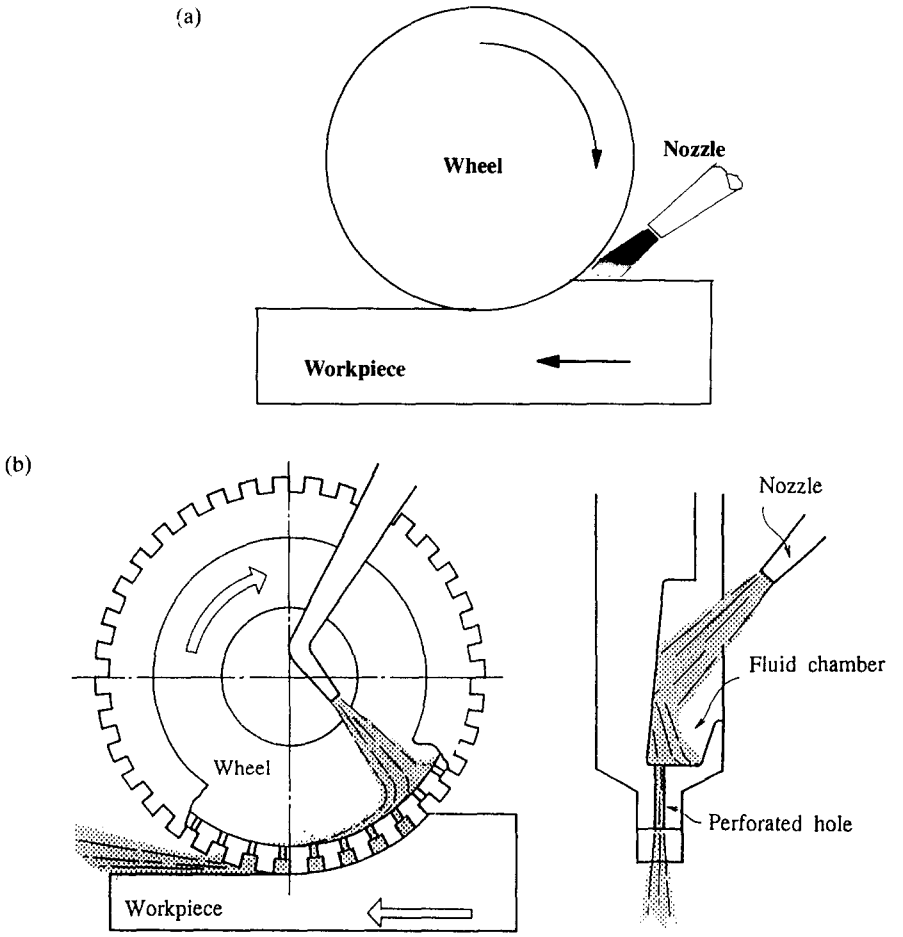

FIG. 2. Wheel structures and coolant supply methods: (a) HA wheel; (b) CBN and MDY wheels.

Wheel dressing was controlled with parameters listed in Table 2. It is well known that a grinding operation is strongly dependent on the initial surface condition of the wheel, which is difficult to control even with the same wheel dressing parameters. To obtain more comparable data for the present study, a more reliable calibration procedure was particularly designed to identify a wheel surface condition after the standard dressing presented in Table 2.

A newly dressed wheel was applied to grind a specified material under a standard

TABLE 2. WHEEL DRESSING CONDITIONS

Dressing procedure	Step 1	Step 2
Type of dresser	Single point diamond dresser (dull)	Single point diamond dresser (sharp)
Radial feed (mm × str)	0.04 × 12 + 0.02 + 1	0.01 × 10
Wheel speed (rpm)	1000	1000
Dressing speed (mm/rev)	0.1	0.1

Dressing procedure	Step 1	Step 2
Type of dresser	GC80HV (Cup type)	WA150HV (Cup type)
Dimension of dresser (mm) (outer diameter × inner diameter)	ϕ 90 × ϕ 50	ϕ 90 × ϕ 50
Wheel speed (m/s)	10	10
Dresser speed (m/s)	2.5	2.5
Transverse table speed (mm/min)	500	500
Radial feed (mm × str)	0.01 × 100	0.03 × 16 + 0.02 × 1

condition (in this study a = 1.0 (mm) and v_w = 1.0 (mm/sec) were adopted in the experiment). The wheel surface was thought of as being identified when all outputs of the calibrating operation, such as grinding forces, surface roughness and grinding power, were approximately coincident with the results of a pre-selected sample, otherwise, the wheel would be dressed again or a further grinding be conducted under the standard conditions.

This calibration procedure in conjunction with the well-controlled standard dressing conditions would produce much more identical surface topography for wheels in the sense of macroscopic reliability.

The horizontal and vertical grinding forces, F_h and F_v, were measured with a dynamometer of KISTLER 5007 in three directions and plotted against grinding time with a YEW 3056 pen recorder. The normal and tangential forces, F_n and F_t were then calculated by:

$$\begin{cases} F_n = F_v\cos\theta - F_h\sin\theta, \\ F_t = F_v\sin\theta + F_h\cos\theta, \end{cases}$$

where $\theta = (a\,D)^{1/2}$ with a standing for the wheel depth of cut and D the diameter of the wheel. The power of the grinding wheelspindle was digitized by a YEW digital AC power meter of type 2503. The surface roughness of ground workpieces and wheel surfaces were traced by TALYSURF 6 and the data were treated by TALYDATA 2010, a program for surface texture analysis. The length of the bulk specimens along the direction of grinding was 100 mm. All measurements of surface texture were conducted in the neighbourhood of the mid-point of the length, where most stable grinding conditions were achieved and maintained during a grinding pass.

3. RESULTS AND DISCUSSION

3.1. *Surface texture analysis*

3.1.1. *Characteristics of the bearing ratio.* The difference between ductile and brittle grinding modes can be clarified, to a great extent, by the comparison of the bearing ratio, t_p, which is a measure of the length of bearing surface, where the profile peaks have been cut off at a line that runs parallel to the mean line of the profile. When this line is set to the height of the largest profile peak, t_p is 0% because no part

of the profile intersects the bearing line. When the line is set to the depth of the lowest profile valley, t_p reaches 100% as all the profile is above the bearing line. Hence, the shape of a t_p curve describes the feature of the peak–valley distribution of a surface. As Fig. 3 shows schematically, the variation of a typical bearing ratio curve is characterized by a steep attenuate region A, a wide gentle reduction region B and a very narrow region C. The number and height distribution of higher peaks determines the slope magnitude and the width of region A. Region B must be wide since the heights of most asperities distribute in a wide range. The slope of the curve indicates the variation of the widths of the asperities. The extremely narrow region C denotes the percentage of deep valleys. If the slope of t_p in region B is very small and if the transition from B to C is sharp, there must exist only few very deep valleys.

In grinding ductile materials, because of plastic ploughing of neighbouring active grains, some peaks with large heights are formed, but the number of such peaks are few; thus they will be represented by a steep but narrow attenuate region A. In grinding brittle materials, however, ploughing cannot result in large plastic flow so that sharp peaks usually do not exist and hence t_p will vary more slowly in region A. Owing to similar reason, the slope magnitude of curve t_p in region B for a ground surface of a ductile material must be much bigger than that of a brittle material. Brittle materials like to break and if the normal force on an active grain is too large lateral cracks will initiate and develop beneath the grain so that a deep pit will be produced owing to the material breakage, which is denoted by the t_p curve with a sharp change from region B to C. The t_p curves of SUJ2, Si_3N_4 and SiC along the grinding direction shown in Fig. 4 strongly confirm the above statements. However, t_p curves in the direction perpendicular to the grinding direction seem to be unable to clearly distinguish these features, probably because of the influence of the existing cutting grooves on a ground surface.

The above distinct observation is useful in the measurement or recognition of grinding brittle materials in the so-called ductile regimes. If a ground surface of a brittle material presents a t_p curve with the characteristics of a ductile material, it may show to a great extent that the grinding mechanism was in a ductile mode.

3.1.2. *Variation of surface roughness.* The characterization of surface roughness (SF) has been a major concern in assessing the surface texture of ground components. A number of parameters have been used to reveal the dependence of the SF upon external as well as internal factors. For all the workpiece materials (SUJ2, SiC and Si_3N_4) used in the present experiment, the SF along both the grinding and its perpendicular directions exhibits simple correlations with the equivalent chip thickness h_{eq} (see Fig. 5):

$$R_a^I = \beta_a^I (h_{eq})^{\alpha^I} \equiv \beta_a^I \left(\frac{v_w a}{v_s}\right)^{\alpha^I}, \qquad (I = A, P) \tag{1}$$

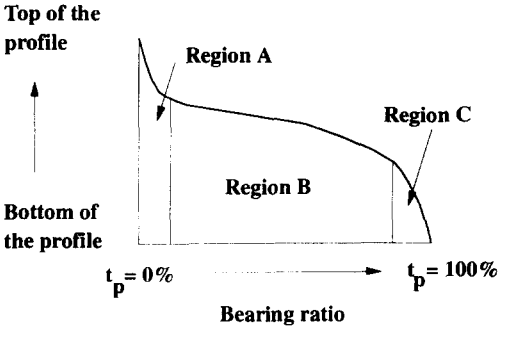

FIG. 3. A schematic diagram of a t_p curve.

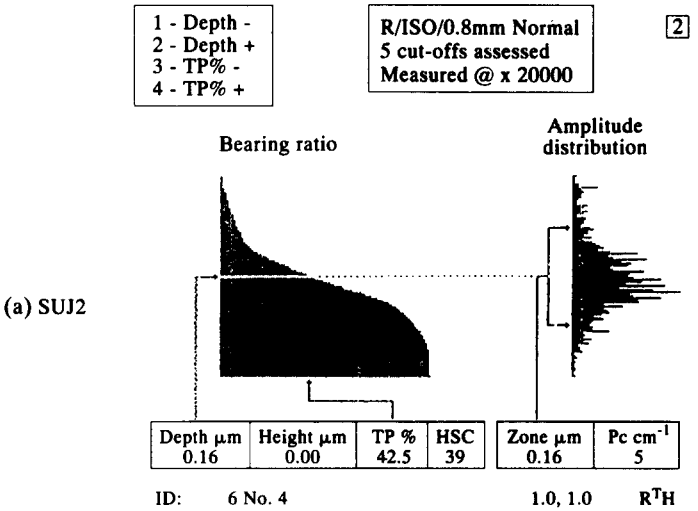

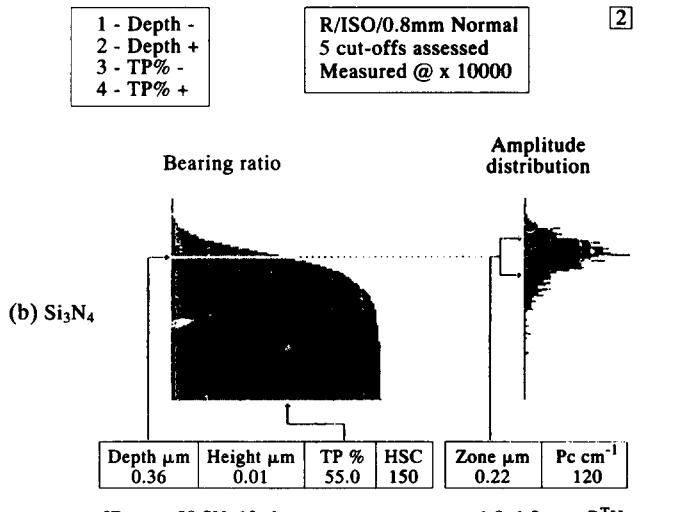

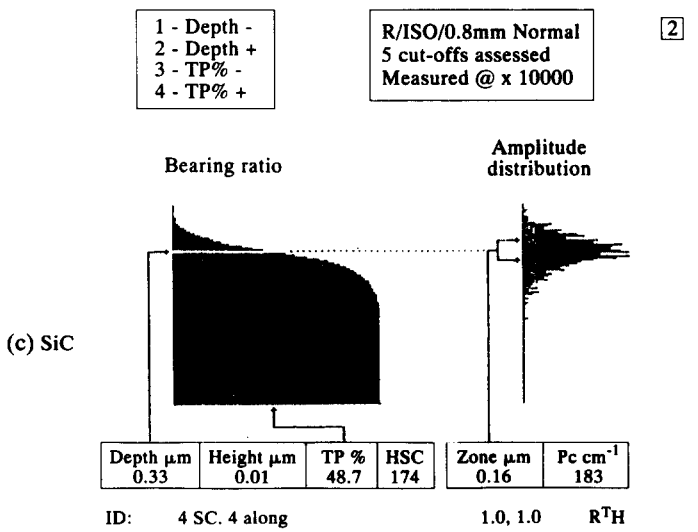

Typical t_p curves

FIG. 4. Typical t_p curves (grinding conditions: a = 1.0 (mm) and v_w = 1.0 (mm/sec)): (a) SUJ2; (b) Si_3N_4; (c) SiC.

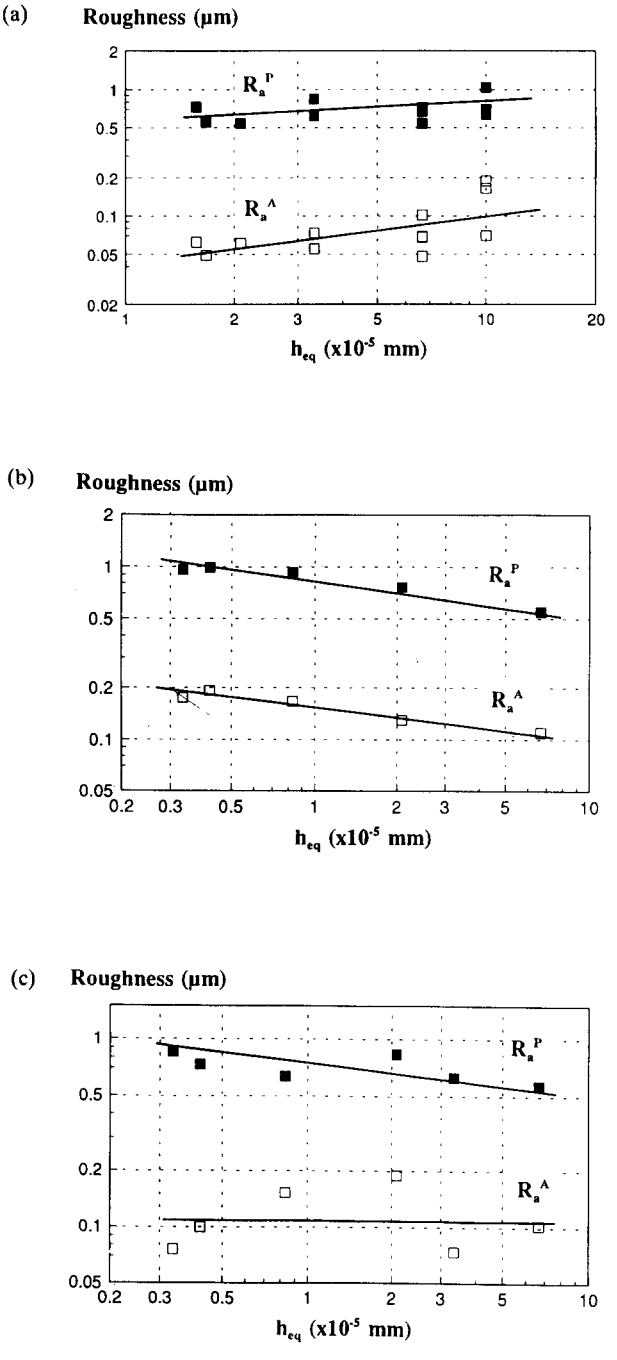

FIG. 5. The correlation of surface roughness with equivalent chip thickness: (a) SUJ2 with CBN wheel; (b) Si_3N_4 with MDY wheel; (c) SiC with MDY wheel.

where β_a^I and α_a^I are constants and could be determined by experimental data, superscript "A" means "along the grinding direction" and "P" "perpendicular to the grinding direction". R_{tm} follows the same formula as equation (1) provided that the subscript "a" in the above equation is replaced by "tm". Equation (1) is in exactly the same form as that for cylindrical grinding [9–10] (see also p. 187 of Ref. [11]). It is of interest to note that for material SUJ2, R_a^I and R_{tm}^I increase with the increment of h_{eq}, which is in agreement with the prediction of Refs [9–10], but for SiC and Si_3N_4 they behave just inversely. This is believed to be related to the different grinding mechanisms of ductile and brittle materials. With the increase of h_{eq}, interface normal and shearing forces increase significantly [12]. This may bring about further growth of ridges in the

formation of grooves in grinding ductile materials. In contrast, such higher interface forces may smooth the ridges through forced breakage during grinding brittle materials.

The above discussion could be further confirmed by comparing the values of the ratios:

$$\zeta_a = \frac{R_a^P}{R_a^A}, \quad \zeta_{tm} = \frac{R_{tm}^P}{R_{tm}^A}. \tag{2}$$

As imagined, in CFG regimes, a ground surface of a ductile material would usually possess higher ridges if compared with that of a brittle material. Thus $\zeta_{ductile}$ should be larger than $\zeta_{brittle}$ generally. The results in Table 3 do show that these values are in very good agreement with what was expected.

It should be mentioned that the morphology of a ground surface could be affected remarkably by the grinding temperature [13]. Accordingly, the parameters, β and α, in equation (1) should be calculated again whenever the cooling condition (type of coolant, coolant supply method, etc.) has been changed. A thorough thermal analysis is necessary to obtain a detailed correlation between the surface morphology and grinding temperature field.

3.2. *Study of grinding forces*

3.2.1. *Force ratios.* The main differences between the forces between grinding metallic and ceramic materials are shown in Fig. 6. For SUJ2, the ratio of normal force F_n to tangential force F_t always remains constant regardless of changes of equivalent chip thickness and the type of the grinding wheels. However, those for SiC and Si_3N_4 present quite strong non-linearity. As has been discussed in Ref. [12], interface forces are built up from the interaction between the workpiece material and the active and inactive grains as well as bond material of the wheel. This, in turn, relates to the chip formation mechanism of the process. For ductile materials, the chip formation is due to plastic shearing flow, thus statistically it could be considered as a stable process because the plastic deformation parameters of the material are constants under stable grinding conditions. This is not true in grinding ceramics. Because of the squeezing between the wheel and workpiece surfaces, the fractured chips may break again into much smaller pieces or particles soon after their first breakage from the bulk. Compared with loaded metallic tape-like chips on the wheel surface, such kinds of particulate chips are more easily released and hence the grinding wheel may show a more obvious self-cleaning process during grinding. The force traces in Fig. 7(a) and (b) clearly show this self-cleaning phenomenon in grinding SiC and Si_3N_4. The time interval $[0,t_1]$ may be thought of as an accumulation period of chip loading with the fact of force arising (wheel wear is negligible in such a short pass). $[t_1,t_2]$ could be called the self-cleaning period when most loaded particulate chips drop off such that grinding forces decrease quickly. A new chip loading process begins at $t = t_2$ signed by the second force climbing. It becomes more clear if these force traces are compared with those of the bearing steel (Fig. 7c) where the grinding force always remains constant. It may argue that the self-cleaning could actually be the self-sharpening of the wheel caused by newly exposed active grains. Indeed these two phenomena would produce similar resultant behaviour on the grinding force traces. Unfortunately, careful microscopic checks of the wheel surface comparison before and after each pass of grinding did not provide

TABLE 3. A COMPARISON OF THE AVERAGE VALUES OF ζ OF DIFFERENT MATERIALS

	SUJ2	SiC	Si_3N_4
ζ_a	11.064	8.661	6.534
ζ_t	14.015	3.661	4.108

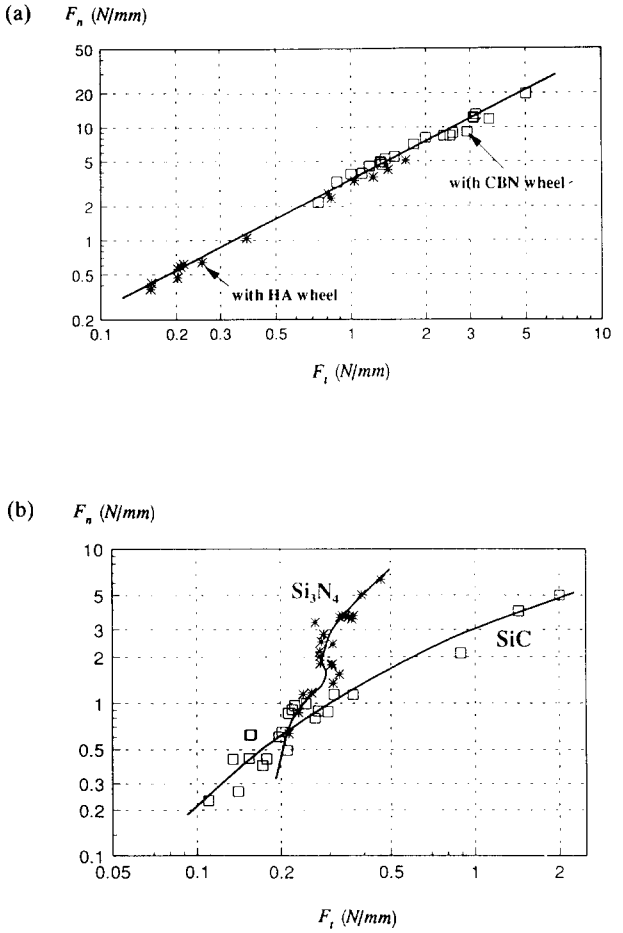

FIG. 6. Variations of normal and tangential grinding forces per unit grinding width, F_n and F_t (N/mm): (a) SUJ2 with CBN and HA wheels; (b) Si_3N_4 and SiC with MDY wheel.

any evidence for the argument. In all the above examples, coolant pressure and flowrate were constant through the grinding processes.

3.2.2. *Formulation of grinding forces.* As the chip formation mechanism of grinding ceramics is brittle fracture, the grinding forces must somehow depend on the fracture toughness of the material. Furthermore, before chipping, the surface material of the workpiece must undergo elastic (even certain constrained plastic) deformation. For simplicity, let us first consider the grinding forces as the simple summation of the forces exerted on individual active grains. This simplification immediately suggests that the problem is extremely related to the processes of single point cutting and indentation of ceramics by harder indenters (for example, diamonds). Accordingly, the grinding forces must also be influenced by the hardness of the workpiece material. On the other hand, it has been found that the normal force causing fracture in a quasi-static indentation test (where the tangential force is zero) is rather different from that in a single point cutting process where the indenter is moving along the material surface (so that the tangential force emerges). Consequently, the depth of cut and the cutting speed should be involved in relation to the resultant forces. Hence, the normal and tangential grinding forces per grinding width could be expressed as:

$$F_{n/t} = f_{n/t}(K_{IC}, H, a, v_w, v_s, b), \tag{3}$$

where b is the grinding width and $F_{n/t}$ means F_n or F_t. In the study of indentation

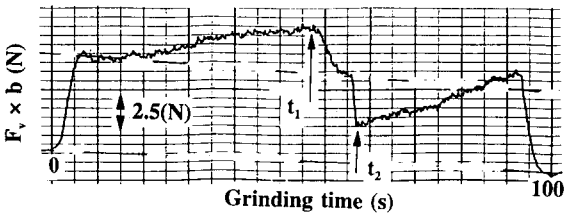

(a) SiC (a = 0.1mm and v_w = 1.0mm/s)

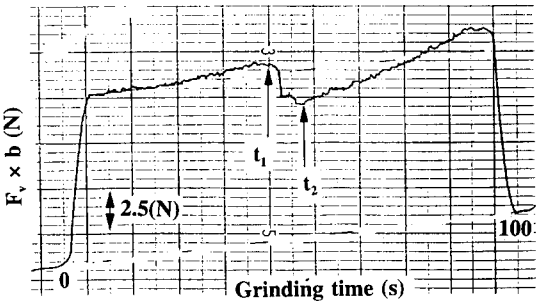

(b) Si_3N_4 (a = 0.1mm and v_w = 1.0mm/s)

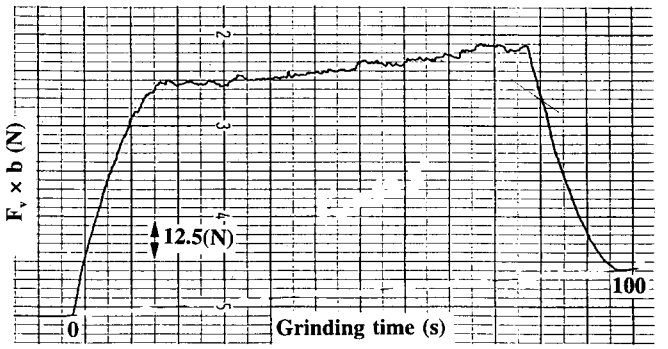

(c) SUJ2 (a = 2.0mm and v_w = 1.0mm/s)

FIG. 7. Typical examples of traces of the vertical grinding force, $F_v b$(N): (a) SiC (a = 0.1 mm and v_w = 1.0 mm/sec); (b) Si_3N_4 (a = 0.1 mm and v_w = 1.0 mm/sec); (c) SUJ2 (a = 2.0 mm and v_w = 1.0 mm/sec).

mechanics [14], it has been found that the critical indentation load of initiating a crack is:

$$P_{\text{critical}} = \gamma \cdot g(E_w/H) \cdot \left(\frac{K_{IC}^4}{H^3}\right), \tag{4}$$

where E_w is the elastic modulus of the workpiece material, γ is a dimensionless constant and $g(E_w/H)$ is only a weak function. The combination term $\lambda = K_{IC}^4/H^3$ is, therefore, a very good parameter for simplifying expression (3). Another combined parameter that involves v_w, v_s and a is naturally the equivalent chip thickness $h_{eq} = av_w/v_s$. Consequently, we may rewrite equation (3) into:

$$F_{n/t} = f_{n/t}(\lambda, h_{eq}, b). \tag{5}$$

Nevertheless, the functional structure of the right hand side of equation (4) does suggest that $F_{n/t}$ may behave as

$$F_{n/t} = \lambda \cdot f_{n/t}(h_{eq}, b), \tag{6}$$

or in a non-dimensional form according to the method of dimensional analysis:

$$\bar{F}_{n/t} \equiv \frac{bH^3 F_{n/t}}{K_{IC}^4} = \bar{f}_{n/t}(\bar{h}_{eq}), \tag{7}$$

where

$$\bar{h}_{eq} \equiv \frac{v_w a}{v_s b} \tag{8}$$

is the non-dimensional equivalent chip thickness. Equation (7) presents the general relationship between the non-dimensional grinding forces and the non-dimensional equivalent chip thickness, and states that all force values of $\bar{F}_n$ or $\bar{F}_t$ for grinding different materials should lie on a single curve if they are plotted in the $\bar{F}_n$–$\bar{h}_{eq}$ or $\bar{F}_t$–$\bar{h}_{eq}$ frame. This conclusion is very well confirmed by the data in grinding SiC and Si_3N_4 in the present experiment. Figure 8 illustrates the fact clearly. Explicit formulae for $\bar{F}_n$ and $\bar{F}_t$ can easily be obtained by using the least squares method.

4. CONCLUSIONS

A number of new findings and insights have been explored from the comparative study of creep-feed grinding metallic and ceramic materials.

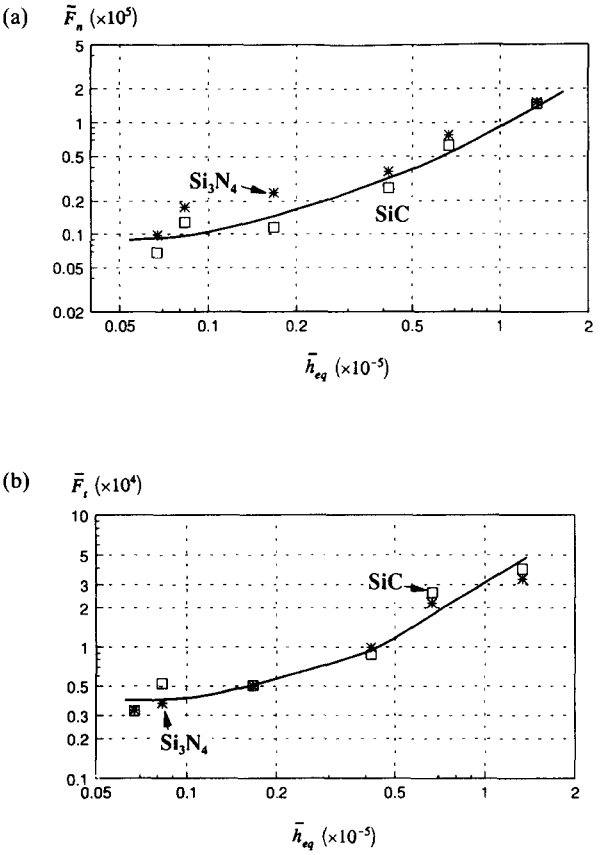

FIG. 8. Grinding forces in the non-dimensional coordinates $\bar{F}_{n/t}$–$\bar{h}_{eq}$: (a) $\bar{F}_n$; (b) $\bar{F}_t$.

(1) the bearing ratio curve of the ground surface of a brittle material may be used to recognize the grinding mechanism, brittle- or ductile-mode mechanism;

(2) the surface roughness for both metallic and ceramic materials follows a simple power relation with respect to the equivalent chip thickness in the form of equation (1). The exponent is positive for metallic materials but negative for ceramics. The parameters, however, need to be calculated again whenever the cooling condition has been changed;

(3) the relationship between the normal and tangential forces in grinding brittle materials is non-linear. A self-cleaning mechanism is proposed to explain this phenomenon and has indirectly been approved by experimental observations; and

(4) a general formula, equation (7), for modelling the grinding forces F_n and F_t has been successfully established, in terms of the hardness and fracture toughness of the workpiece material and the equivalent chip thickness of the grinding operation.

The above conclusions, especially the simple formulae of surface roughness and grinding forces, could easily be used in practice.

Acknowledgments—The financial support from the Australian Research Council Small Grant Scheme and the discussion and experimental assistance from Dr T Suto and H. Noguchi are appreciated.

REFERENCES

[1] L. C. Zhang, T. Suto, H. Noguchi and T. Waida, An overview of applied mechanics in grinding. *Manufac. Rev.* **5**, 261 (1992).
[2] C. Andrew, T. D. Howes and T. R. A. Pearce, *Creep Feed Grinding*. Industrial Press, New York (1985).
[3] J. Yoshioka, F. Hashimoto, M. Miyashita, A. Kanai, T. Abo and M. Daito, Ultraprecision grinding technology for brittle materials: application to surface and centerless grinding processes, in *Milton C. Shaw Grinding Symposium*, edited by R. Komanduri and D. Maas, ASME Production Engineering Division, **16**, p. 209 (1985).
[4] T. G. Bifano, T. A. Dow and R. O. Scattergood, Ductile-regime grinding: a new technology for machining brittle materials. *Trans. ASME. J. Engng Ind.* **113**, 184 (1991).
[5] I. D. Marinescu and J. A. Webster, Brittle/ductile grinding of soft basalt ceramics, *ASPE Spring Topical Meeting on Principles of Cutting Mechanics*, Tucson, Arizona, 13–15 April (1993).
[6] M. J. Ball, N. A. Murphy and P. Shore, Electrolytically assisted "ductile" mode diamond grinding of BK7 and SF10 optical glasses, *SPIE Procs Commercial Applications of Precision Manufacturing at the Sub-Micron Level*, SPIE Vol. **1573**, Society of Photo-Optical Instrumentation Engineers, Washington, p. 30 (1991).
[7] A. G. Atkins and Y.-W. Mai, *Elastic and Plastic Fracture*. Ellis Horwood, Chichester (1988).
[8] T. Suto, T. Waida, H. Noguchi and H. Inoue, High performance creep feed grinding of difficult-to-machine materials with new-type wheels, *Bull. Jpn Soc. Prec. Engng* **24**, 39 (1990).
[9] R. Snoeys *et al.*, The significance of chip thickness in grinding, *Ann. CIRP* **23**, 227 (1974).
[10] S. M. Kedrov, Investigation of surface finish in cylindrical grinding operations, *Mach. Tool.* **51**, 40 (1980).
[11] S. Malkin, *Grinding Technology: Theory and Applications of Machining with Abrasives*. Ellis Horwood, New York (1989).
[12] L. C. Zhang, T. Suto, H. Noguchi and T. Waida, Applied mechanics in grinding, Part II: Modelling of elastic modulus of wheels and interface forces, *Int. J. Mach. Tools Manufact.*, **33**, 245 (1993).
[13] A. Hosokawa, H. Yasui and K. Higuchi. Influence of wet grinding temperature on surface morphology of fine ceramics, *Proc. ASPE 1993 Annual Meeting*, Seattle, Washington, 7–12 November (1993).
[14] A. G. Evans and D. B. Marshall, Wear mechanisms in ceramics, in: *Fundamentals of Friction and Wear of Materials*, edited by D. A. Rigney, *American Society for Metals*, Ohio, p. 439 (1981).